INFLUENCE OF CHEMICAL COMPOSITION OF MICROALLOYED STEEL AND COOLING RATE OF HAZ METAL OF PIPE WELDED JOINTS ON ITS STRUCTURE AND IMPACT TOUGHNESS

A.A. RYBAKOV, T.N. FILIPCHUK, V.A. KOSTIN and **V.V. ZHUKOV**
E.O. Paton Electric Welding Institute, NASU
11 Bozhenko Str., 03680, Kiev, Ukraine. E-mail: office@paton.kiev.ua

One of the most difficult tasks in manufacture of the gas-and-oil line pipes, from the point of view of technology of their welding, is fulfillment of the requirements of normative indices on impact toughness of HAZ metal of welded joint. The aim of present work is an investigation of effect of chemical composition of microalloyed steel and cooling rate of HAZ metal of pipe welded joints on its structure-and-phase state and toughness characteristics. Specimens of Kh70 grade steel of different chemical composition varying, mainly, in carbon content and different rate cooling conditions simulating HAZ metal of the pipe welded joints were studied using modern Gleeble-3800 complex. It is determined that a structure of bainite type, i.e. lamellar ferrite with strengthening second phase martensite-austenite-carbide — MAC or carbide phase), is mainly formed in the metal of studied chemical composition in sufficiently wide interval of the cooling rates. Density of distribution of the phase, its location (orientation), dimensions and morphology are determined, in preference, by chemical composition, and, to lesser degree, by metal cooling rate of the $V_{cool.8/5}$. In this connection, the possibilities of metallurgical factor influence should be use to greater extent in order to increase HAZ metal toughness. Strict limitation of weight fractions of the elements promoting formation of coarse ferrite packages with ordered carbide phase of lamellar morphology (for example carbon, niobium, molybdenum etc.) is also reasonable for formation of optimum structure and, respectively, improvement of HAZ metal toughness together with reduction of content of the detrimental impurities in steel (sulfur, phosphor and nitrogen) to minimum possible level. The results of investigations were used in production of pipes from low-alloyed steel of Kh70 grade for main gas-and-oil pipelines. 10 Ref., 3 Tables, 6 Figures.

Keywords: *microalloyed steel, welded joint, heat-affected zone, cooling rate, microstructure, impact toughness*

In recent time, a complex of requirements to pipes, including impact toughness of metal of the welded joints [1, 2], is continuously restricted due to necessity of providing of safe operation of the main pipeline systems used for transportation of liquid and gaseous carbohydrates. It is well known fact that large diameter welded pipes from high-strength microalloyed steels [3] are mainly used for such pipelines. Analysis of current normative documents, literature data and own investigations indicates that one of the most complex problems in the manufacture of gas-and-oil line pipes, from point of view of technology of their welding, is fulfillment of the normative indices on impact toughness of metal of welded joint heat-affected zone (HAZ).

Many researchers [4, 5] note a significant spread of impact toughness values in testing of HAZ metal of the welded joints from modern pipe steels that is caused by series of factors, i.e. structural heterogeneity of welded joints, notch location, metal structure state, in particular, adjacent to the notch, configuration of fusion line, portion and properties of the weld metal and different HAZ areas in fracturing section, reaction of steel on thermal-deformation welding cycle, etc.

Structural state of HAZ metal is one of the determining factors, affecting its impact toughness. Different structure areas of the welded joint, including coarse grain area of reduced toughness (local embrittlement zone — LEZ) adjacent to the fusion line, are incorporated in test section at any scheme of applying of the notch for evaluation HAZ metal toughness regulated by normative documents. Ductile characteristics of metal of HAZ near-weld area significantly [6–8] are reduced by considerable growth of austenite grain in LEZ, observed in welding, formation of large packages of lamellar ferrite, upper bainite and presence of martensite-austenite-carbide (MAC) phase. Dimensions, microstructure and properties of a welded joint area

with reduced toughness are determined by chemical composition of base metal and welding conditions (including metal cooling rate in temperature range of possible transformations, i.e. 800–500 °C). This area, in particular, has a decisive effect on integral index of impact toughness at HAZ metal testing.

LEZ area in the real welded joints has complex configuration and relatively small dimensions due to which the evaluation of impact toughness, particularly of this area, and its role in the integral toughness index is complicated. At the same time, the information about structure and metal properties in LEZ is very important for solving the task of providing of required welded joint ductile characteristics. From this point of view, the investigations applying the methods of physical modelling of metal structure transformations in welding, in particular, on modern complex Gleeble-3800 [9], which was used in the present work, are the most correct.

Aim of the work lied in the investigation of effect of chemical composition of microalloyed pipe steel and metal cooling rate on structure-phase characteristics of the metal in area of coarse grains in welded joint HAZ. The specimens, cut from steel of 25–33 mm thickness across the rolling direction (cylinder of 10 mm diameter or rectangular of 10 × 10 mm section), were heated around 40 °C/s rate. The maximum heating temperature of the specimens in simulation of the welding cycles made 1300 °C, time of holding at this temperature 1s. In these investigations the cooling rate of metal of tested specimens in 800–500 °C ($V_{cool.8/5}$) range was selected from the modes of submerged multiarc welding used in reality for manufacture of large diameter longitudinal welded pipes. Calculation of $V_{cool.8/5}$ for typical modes of five-arc welding of outside welds of the pipes with 22–36 mm wall thickness under condition of initial temperature of welded edges in the range from 20 up to 100 °C (increased initial temperature of the edges under conditions of continuous pipe production is possible due to insufficient time interval between the end of welding of inside weld and beginning of performance of outside weld) was carried out for determination of the limits of this parameter change. Well-known formula [10] was used in the calculation using which a time of metal staying in the indicated range $t_{8/5}$ was determined:

$$t_{8/5} = \frac{\eta^2}{4\pi\lambda\rho c}\left(\frac{UI}{V}\right)^2 \frac{1}{d^2}\left[\left(\frac{1}{500 - T_0}\right)^2 - \left(\frac{1}{800 - T_0}\right)^2\right],$$

where η is a welding heat efficiency, taken equal 1 for submerged arc welding; λ is a coefficient of thermal conductivity of steel, equal $3.8 \cdot 10^{-4}$ kJ/cm·s·deg; ρ is a steel density, g/cm^3; c is a specific thermal capacity of steel, J/g·deg; $\rho c = 0.005$ kJ/cm^3·deg; d is a sheet thickness, cm; T_0 is an initial metal temperature before welding; UI/V is a heat input of five-arc welding process.

Respectively, cooling rate $V_{cool.8/5}$ of the metal was determined as a value inverse to time of its staying in 800–500 °C temperature range.

According to the calculations the rate of metal cooling $V_{cool.8/5}$ makes 7.2–4.5 °C/s in submerged multiarc welding of pipes with 22–36 mm wall thickness at different initial temperature of welded edges (from 20 to 100 °C). Based on this data the time of metal staying in the indicated temperature range during welding thermal cycle simulation were set equal 45, 50 and 55 s that corresponds to cooling rate 6.7, 6.0 and 5.4 °C/s. Separate specimens of steel were cooled with lower (3 °C/s) or larger (12 and 30 °C/s) rate, at the $t_{8/5}$ made 100, 25 and 10 s, respectively.

Reaction of different origin K60 (Kh70) grade steel on thermal cycle of multiarc welding was investigated. This steel grade is used in production of the pipes for main gas-and-oil pipelines and conventionally marked by letter indices from A to D. Studied metal (Table 1) on chemical composition represents itself silicon-manganese steel with ultra-low content of detrimental impurities (in particular, weight fraction of sulfur made 0.001–0.002 %, phosphor was 0.008–0.012 % and content of nitrogen did not exceed 0.006 %), microalloyed by niobium (0.038–0.054 %) and vanadium (0.032–0.040 %, except

Table 1. Chemical composition of studied steels, wt.%

Symbolic key of the specimen	C	Mn	Si	P	S	Ni	Ti	Mo	Nb	V
A	0.032	1.79	0.27	0.011	0.001	0.21	0.019	< 0.03	0.050	0.032
B	0.045	1.79	0.23	0.012	0.002	0.21	0.013	< 0.03	0.054	0.038
C	0.080	1.62	0.11	0.014	0.002	0.23	0.012	< 0.03	0.038	< 0.02
D	0.076	1.53	0.26	0.008	0.002	0.20	0.013	0.11	0.043	0.040

for C grade steel specimens, in which weight fraction of vanadium is lower than 0.02 %). Quantity of manganese in the studied metal was in relatively narrow limits (from 1.53 to 1.79 %). The most significant differences in chemical composition of the examined metal lied in carbon content which changed in the ranges from 0.032 to 0.080 %. Examined specimens of steel can be divided into two groups on content of this element, i.e. with low content of carbon (0.032–0.045 % C, symbolic keys A and B) and with increased content of carbon (0.076–0.080 %, keys C and D). It should be noted that steel D, containing 0.076 % of carbon, was additionally microalloyed, except for niobium and vanadium, by small quantity of molybdenum, weight fraction of which made 0.11 %. The weight fraction of niobium (0.050–0.054 %) is somewhat larger in low-carbon steel A and B.

Kinetics of structural transformation of the metal of examined steel specimens (temperature of beginning T_b and ending T_e) at different rate of their cooling in 800–500 °C range were determined by analysis of heating and cooling dilatograms (Table 2).

As it was expected, increase of time of metal staying in 800–500 °C temperature range (reduction of cooling rate) rises the temperature of beginning and ending of transformation for all examined specimens, however these changes are not so significant. In this connection, sufficiently high structural stability of the examined steels, in particular steel D, additionally microalloyed by small quantity of molybdenum, should be noted. Thus, metal with carbon low content (specimens A and B) lies in 656–696 °C limits in $t_{8/5}$ range from 10 to 45 s ($V_{cool.8/5}$ from 30 up to 6.7 °C/s) and steels with increased carbon content (specimens C and D) belong to 640–657 °C. At that T_b of steel D, containing 0.11 % of molybdenum, does not virtually change in the indicated range of cooling rate and makes 656–657 °C. The same dependence on cooling rate was also determined for temperature of ending of metal structural transformations (Table 2) during investigations.

The following can be noted when analyzing the results of determination of T_b and T_e of different chemical composition steel under conditions of change of cooling rate. T_b and T_e of the examined steel specimens, virtually, do not change and to larger extent depend on chemical composition of steel (Figure 1) in the range of cooling rate $V_{cool.8/5}$ = 6.7–5.5 °C/s, corresponding to technical feasibility of its regulation under conditions of traditionally used submerged multiarc double-sided welding of pipe, including from heavy-wall metal. Thus, T_b of steel with reduced carbon content (specimens A and B) lies in the range 700 °C (695–702 °C) and T_e is around 500 °C (499–512 °C) at the indicated range of cooling rate. Respectively, T_b of steel with high content of carbon (specimens C and D) makes 645–600 °C and T_e is 432–492 °C. Minimum temperature of beginning and ending of transformation during the whole studied range of cooling rate is typical for steel with 0.076 % carbon, microalloyed by niobium, vanadium and small quantity of molybdenum (specimen D).

Table 2. Temperature of beginning and ending of austenite transformation in metal of the examined steel specimens at different cooling rate

Symbolic key of the specimen	$t_{8/5}$, s ($V_{cool.8/5}$, °C/s)	T_b, °C	T_e, °C
A (0.032 % C)	10 (30.0)	664	439
	25 (12.0)	671	456
	45 (6.7)	696	499
B (0.045 % C)	10 (30.0)	656	453
	25 (12.0)	682	485
	45 (6.7)	695	509
	50 (6.0)	700	510
	55 (5.5)	702	512
C (0.080 % C)	45 (6.7)	650	480
	50 (6.0)	659	491
	55 (5.5)	660	492
	100 (3.0)	707	500
D (0.076 % C)	25 (12.0)	656	432
	45 (6.7)	657	435
	50 (6.0)	659	440
	55 (5.5)	660	445
	100 (3.0)	670	450

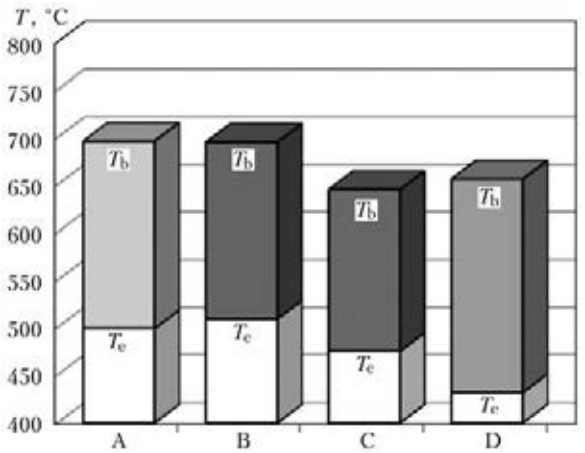

Figure 1. Temperature of beginning T_b and ending T_e of $\gamma \rightarrow \alpha$-transformation of metal of examined specimens at cooling rate $V_{cool.8/5}$ = 6.7 °C/s

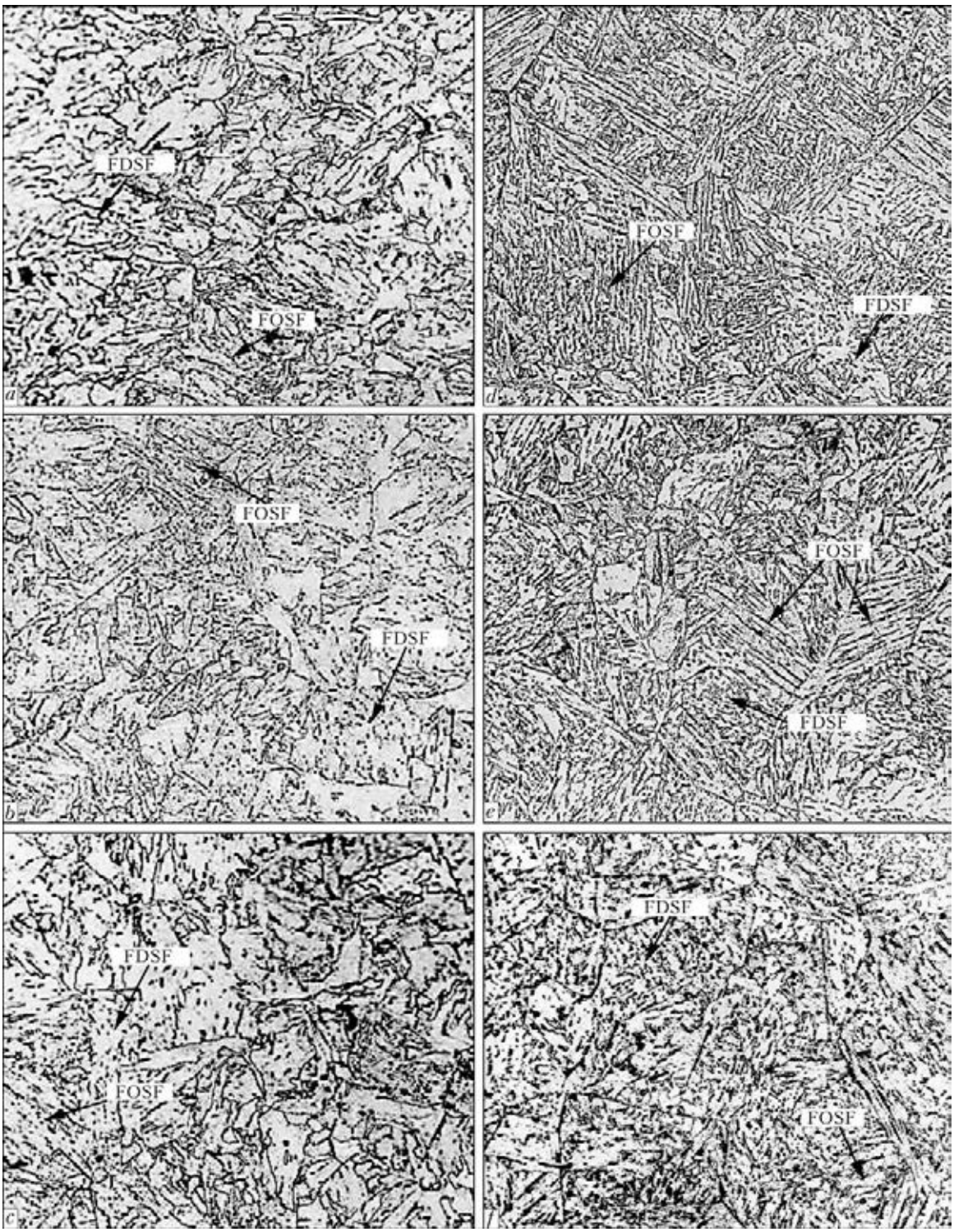

Figure 2. Microstructure (×400) of metal of HAZ simulated specimens (optical microscopy). Specimen A: $V_{cool.8/5}$ = = 6.7 °C/s (*a*); 12 (*b*); 30 (*c*). Specimen C: $V_{cool.8/5}$ = 6.7 °C/s (*d*); 12 (*e*); 30 (*f*). Ferrite with disordered second phase — FDSF, ferrite with ordered second phase — FOSF

Methods of optical and scanning metallography were used for investigation of peculiarities of structural characteristics of the metal of different chemical composition steel after thermal welding cycle simulation with different cooling rate. Microsections of cylinder and rectangular steel specimens were studied after etching in 4 % alcoholic solution of nitric acid (nital).

Coarse grain (number 4 on GOST 5639) structure of lamellar ferrite with sufficiently coarse carbon second phase (MAC-phase or carbide), mainly similarly oriented and normalized (Figure 2, *d* and 3, *a*), is formed in the metal with carbon weight fraction 0.08 % (steel B specimens) at cooling rate typical for HAZ metal of the welded joints of pipes with 25–36 mm wall

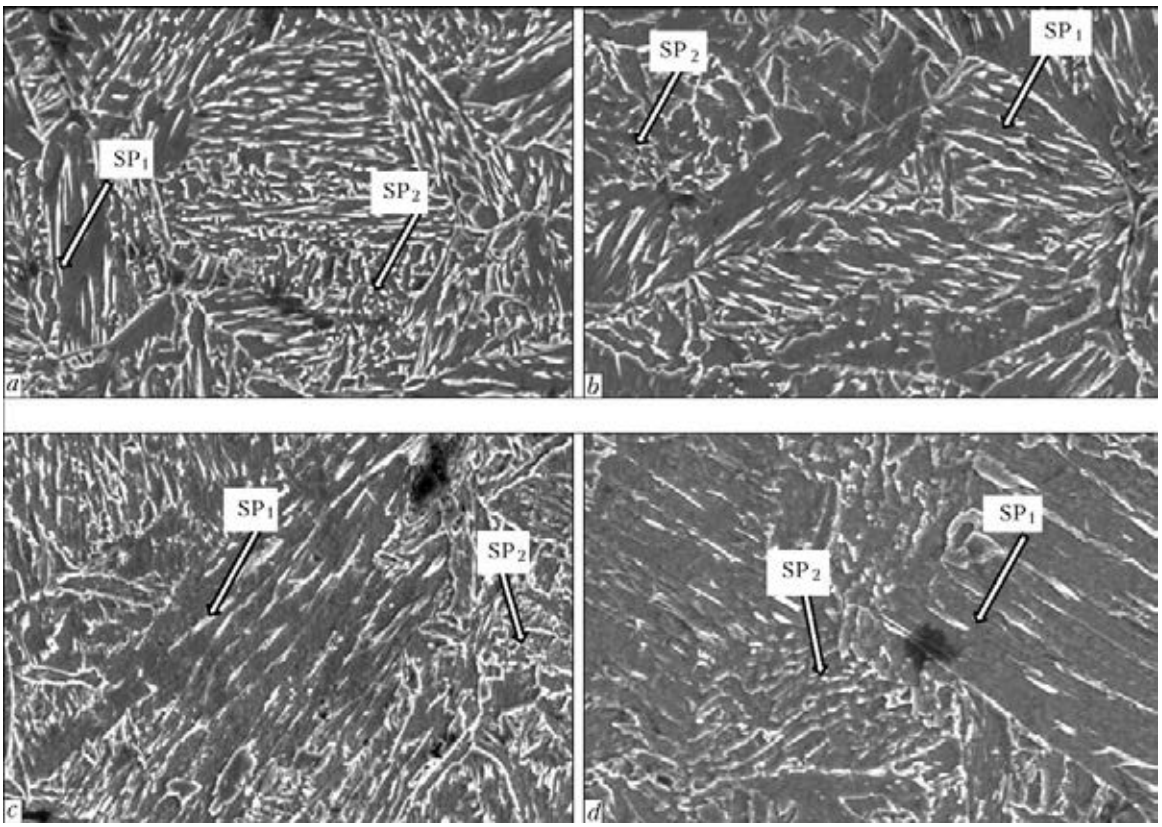

Figure 3. Microstructure of studied specimens of steel after welding thermal cycle simulation (scanning microscopy): *a*, *b* — $V_{cool.8/5}$ = 6.7 °C/s (*a* — specimen C; *b* — specimen D); *c*, *d* — specimen B (respectively $V_{cool.8/5}$ = 6.7 and 12 °C/s); SP_1, SP_2 are second phase of lamellar and grain morphology, respectively

thickness ($V_{cool.8/5}$ = 5.5–6.7 °C/s). It should be noted that majority of coarse grains was fragmented on separate subgrains that clearly determined by dimension and orientation of the second phase precipitations. Second phase, mainly of elongated (lamellar) morphology, is sufficiently tightly distributed in the ferrite matrix (Figure 2, *d* and 3, *a*). Increase of $V_{cool.8/5}$ of the metal above indicated limit (up to 12 °C/s) promotes some increase of dispersion and reduction of volume fraction (distribution density) of the second phase (Figure 2, *e*). The grains, sizes of which correspond to number 4-5 on GOST 5639, are also fragmented. Individual formations of grain morphology, including chaotically located (disordered) ones, are observed together with second phase of elongated form. More dispersed microstructure, representing itself ferrite with tightly located ordered (around 50 %) and disordered second phase mainly of grain morphology (Figure 2, *f*), is formed at cooling rate 30 °C/s. A fringe of hypoeutectoid polygonal ferrite (Figure 4, *a*) is observed along the boundaries of former austenite grain, except for coarse packages of ferrite with ordered second phase of lamellar morphology, at reduction of metal cooling rate $V_{cool.8/5}$ up to 3 °C/s (that is possible, for example, under condition, if initial temperature of the welded edges before performance of pipe outside weld equals approximately 150 °C) in the steel with carbon content 0.080 % (specimens C).

Similar dependence of the structural parameters at change of cooling rate $V_{cool.8/5}$ is also observed in the specimens with smaller content of carbon (specimens A and B, Figure 2, *a*–*c*; 3, *c*–*d*; 4, *b*) as well as in steel with 0.076 % carbon weight fraction and additionally microalloyed by small quantity of molybdenum (specimens D). At that, quantity of carbon structural constituent (MAC-phase) is significantly lower in the structure of simulated HAZ of low-alloy steel (specimens A and B), regardless higher content of niobium which can promote formation of the coarse bainite packages. Formation of MAC-phase in HAZ metal of this steel is more dispersed and, mainly, has grain morphology and their similar orientation is weakly expressed.

It should be noted that microstructure of metal specimens simulating welding thermal cycle with cooling rate around $V_{cool.8/5}$ = 6.7 °C/s, is very close to metal structure in area of coarse grain HAZ of the pipe welded joints, manufactured from steel of corresponding chemical composition (Figure 5).

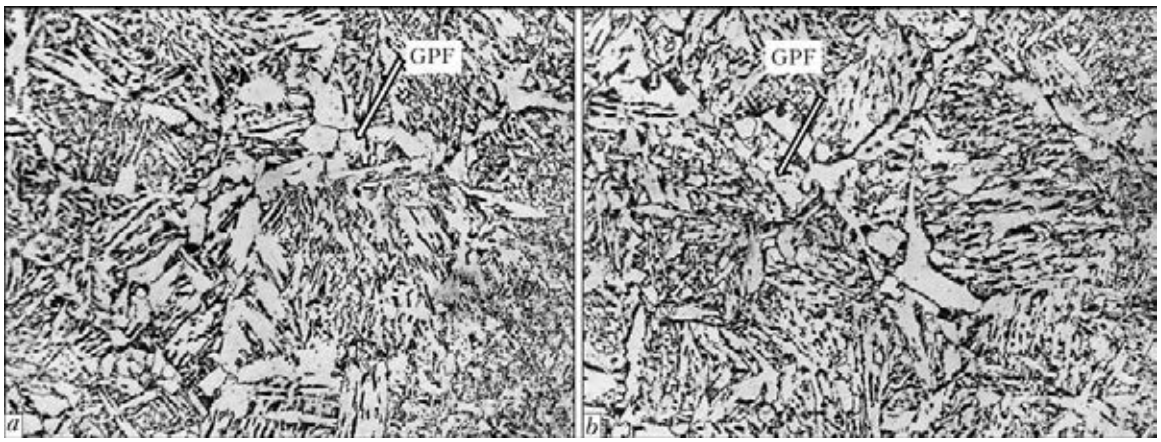

Figure 4. Microstructure (×400) of metal of simulated HAZ specimens with delayed cooling rate ($t_{8/5}$ = 100 s, $V_{cool.8/5}$ = = 3 °C/s): *b* — B (GPF — grain-boundary polygonal ferrite)

Effect of chemical composition on structural state of the metal of simulated HAZ is more significant than changing of the cooling rate in the investigated limits. Dependence of volume fraction (distribution density) of MAC-phase and its morphology on the content of carbon in steel was uniquely determined. Lower quantity of MAC-phase and preferential formation of ferrite grains with MAC-phase of grain type and its chaotic (disordered) distribution were determined in the metal with reduced carbon quantity. Thus, for example, the metal structure of A and B specimens (weight fraction of carbon 0.032 and 0.045 %, respectively) at all investigated $V_{cool.8/5}$ represents itself, mainly, ferrite with dispersed chaotically located carbon phase (MAC-phase, carbides) in preference of grain morphology (Figure 2, *a–c* and 3, *c–d*) and similar grain orientation of dispersed second phase is observed only in separate grains. Volume fraction (distribution density) of second phase in the metal of indicated specimens is significantly lower than in steel with higher carbon content (for comparison, see Figure 3, *a*, *c*).

Increase of weight fraction of carbon up to 0.080 % in steel rises volume fraction (distribution density) of MAC-phase particles in metal structure. At that, MAC-phase has mainly similar orientation (oriented) and, as a rule, lamellar morphology (Figure 2, *d–f* and 3, *a*).

Additional alloying of steel with 0.076 % carbon by molybdenum in 0.11 % quantity promoted some refining of MAC-phase, however, did not result in significant improvement of structural characteristics of the metal in HAZ.

Thus, metallographic investigations showed that structure of bainite type, i.e. lamellar ferrite with strengthening second phase (MAC- or carbide phase) are mainly formed in the metal of studied specimens in sufficiently wide range of cooling rate changing at 800–500 °C temperature. The phase distribution density, location (orientation), sizes and morphology are determined in preference by chemical composition, and to smaller extent, by cooling rate $V_{cool.8/5}$ (in the investigated range). The structure representing itself large packages of lamellar ferrite with similarly oriented second phase, mainly, of elongated shape, is formed in steel with 0.08 % weight fraction of carbon at the cooling rate close to the rate of metal cooling in welding of load bearing pipe welds (approximately 6.7 °C/s). Reduction of carbon content up to 0.032–0.045 % promotes significant reduction of distribution density and

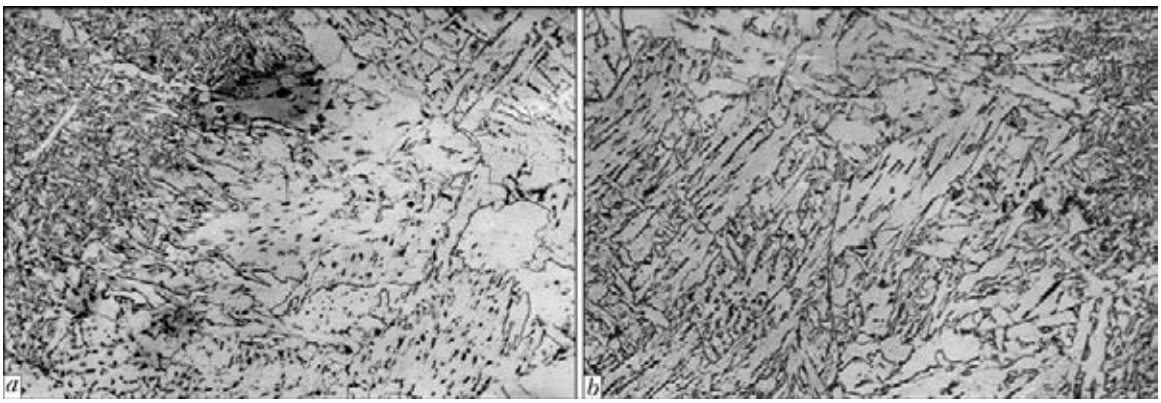

Figure 5. Microstructure (×400) of metal in area of coarse grain HAZ of pipe welded joints from Kh70 steel of different chemical composition: *a* — steel; *b* — B

Table 3. Impact toughness of metal of simulated HAZ specimens of welded joints

Symbolic key of the specimen (carbon content)	$V_{cool.8/5}$, °C/s	KCV, J/cm^2, at T, °C		
		−30	−20	−10
A (0.032 % C)	6.7	38.9; 46.7; 48.2 / 44.6	29.2; 45.8; 54.2 / 43.1	119.5; 125.8; 132.4 / 125.9
	12	41.5; 60.4; 61.2 / 54.4	39.5; 62.8; 77.3 / 59.9	120.4; 134.5; 178.7 / 144.5
	30	41.7; 59.9; 60.1 / 53.9	49.0; 62.9; 79.5 / 63.8	122.4; 135.2; 187.6 / 148.4
C (0.080 % C)	6.7	22.4; 25.8; 29.4 / 25.9	22.2; 31.6; 35.2 / 29.7	51.5; 55.8; 60.4 / 55.9
	12	30.8; 30.9; 35.2 / 32.3	30.7; 33.9; 50.1 / 38.2	51.0; 61.3; 70.1 / 60.8
	30	25.4; 22.8; 31.6 / 26.6	40.1; 41.5; 50.0 / 43.9	57.4; 57.7; 64.3 / 59.8
D (0.076 % C)	6.7	31.4; 34.5; 35.8 / 33.9	33.7; 35.3; 38.5 / 35.8	58.5; 68.3; 70.6 / 65.8
	12	40.2; 41.4; 42.9 / 41.5	42.4; 49.8; 52.9 / 48.4	85.1; 87.4; 95.7 / 89.4

Note. Unit values are indicated in a numerator, and average ones in a denominator.

increase of carbon phase dispersion. At that, the dispersed MAC-phase, mainly of grain morphology, is chaotically located. Such structure characteristics of metal from point of view of its impact strength are more preferable. Significant increase of dispersion and change of distribution density and morphology of MAC-phase in structure of the examined specimens with 0.08 % carbon content was observed only at increase of cooling rate $V_{cool.8/5}$ up to 30 °C/s. However, indicated cooling rate is out of the technical capabilities in submerged multiarc double-pass welding of gas-and-oil line pipes, in particular, with increased wall thickness.

Results of impact bending tests of 10 × 10 mm size specimens with sharp notch, simulating coarse grain area of HAZ of the pipe welded joints, shown in Table 3, well agree with the determined peculiarities of structural characteristics of metal. Thus, changing of cooling rate $V_{cool.8/5}$ in the studied range did not have significant influence on KCV value. For example, the average values of impact toughness KCV of steel C with 0.08 % C changed from 55.9 to 59.8 J/cm^2 at testing temperature minus 10 °C, from 29.7 to 43.9 J/cm^2, at minus 20 °C and 25.9 up to 26.6 J/cm^2 at minus 30 °C, i.e. not more than per 14 J/cm^2 with increase of $V_{cool.8/5}$ from 6.7 to 30 °C/s. Such an insignificant difference of the toughness indices was also observed at change of cooling rate of steel specimens with lower carbon content (Table 3, steel A).

Chemical composition of steel, and, first of all, carbon content had more influence on impact toughness of the metal of simulated HAZ as well as on its structure-phase state. The average KCV value at minus 10 °C made only 55.9 J/cm^2 for specimens of steel C (0.08 % C) which were cooled with 6.7 °C/s rate (typical for submerged multiarc pipe welding). Under the same conditions KCV_{-10} equaled 125.9 J/cm^2 on steel A (0.032 % C) specimens. Reduction of testing temperature up to minus 20 °C and minus 30 °C promoted decrease of level of KCV values of simulated HAZ metal. However, stated dependence on carbon content was preserved.

As fractography investigation showed, all tested impact specimens (from steel of different chemical composition and cooled with various speed) were fractured on quasi-brittle mechanism at temperature minus 30 °C, except for small region under the notch with ductile pit character of rupture (Figure 6, *a*, *c*).

Dimension of facets of quasi-cleavage made in preference 20–70 μm, that approximately corresponds to dimensions of the substructure formations of number 4 fragmented grains, observed in the metal during metallographic investigations (Figure 6, *e*, *h*).

Rupture surface of the specimens was etched in nital (for determination of configuration of MAC-phase particles) with the purpose of evaluation of MAC-phase effect (its sizes and morphology) on fracture character during impact bend testing. As was showed by investigations

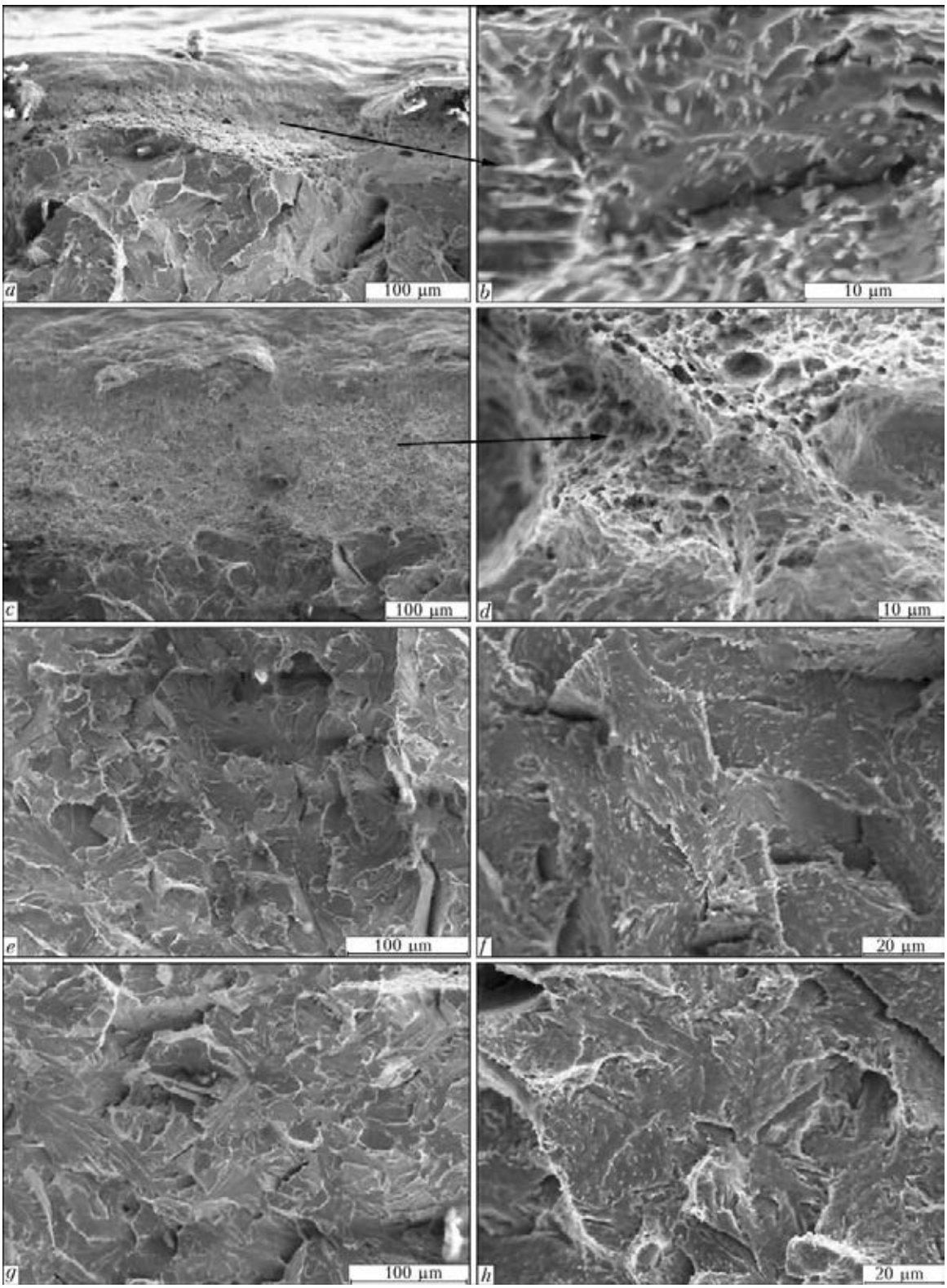

Figure 6. Typical fractogramms of fracture: specimen C — ductile part under notch (*a* — unetched; *b* — after etching); quasi-cleavage area (*e* — unetched; *f* — after etching); specimen A — ductile part under notch (*c* — unetched; *d* — after etching); quasi-cleavage area (*g* — unetched; *h* — after etching)

of these specimens, significant quantity of small fragmented particles of MAC-phase is observed inside the pits in ductile part of the rupture of steel specimens with increased carbon content (specimens C, Figure 6, *b*). Sizes and quantity of such particles is significantly lower (Figure 6, *d*) in steel with 0.032 % C (specimens A). Only small amount of sufficiently dispersed MAC-phase particles are found on the surface of quasi-cleavage facets. Their density distribution and morphology had not significant difference (Figure 6, *f*, *h*) in steel specimens with various carb-

on content. Meanwhile, metallographic investigations determined a sufficiently precise dependence between the quantity and morphology of MAC-phase precipitations and the carbon content in steel (see, for example, Figure 3, *a*, *c*).

Similar indices of metal impact toughness and fracture character of the specimens, simulating HAZ, were registered also at minus 20 °C temperature. Specimens A with low carbon content fractured, mainly, on ductile mechanism at minus 10 °C temperature, when, as it was noted, difference in the impact toughness values of metal of simulated HAZ for steel of different chemical composition is the largest. Portion of ductile fracture in the specimens with high carbon content (steel C, 0.080 % C) did not exceed 40 %.

Results of impact bending tests and fractographic investigations of fractured specimen rupture surface allow assuming that the peculiarities of MAC-phase particle precipitations (density of their distribution, sizes and morphology) affect the energy of ductile fracture to larger extent promoting formation of microvoids and their further coalescence during deformation. Influence of MAC-phase particles is less expressed at brittle fracture.

Conclusions

1. Specimens of steel with different chemical composition, simulating HAZ of the pipe welded joints and differing, in preference, by carbon content, were studied under conditions of metal cooling with different rate. It was stated that structure of bainite type, i.e. lamellar ferrite with strengthening second phase (MAC- or carbide phase) is, mainly, formed in the metal of investigated chemical composition in sufficiently wide range of cooling rates. Density distribution, location (orientation), sizes and morphology of the phase are determined, in preference, by chemical composition, and, to a lesser degree, by metal cooling rate $V_{cool.8/5}$ in the investigated range.

2. Technological capabilities of changing of welded joint cooling rate in multiarc double-pass welding of pipe, in particular, with increased wall thickness are limited. Therefore, increase of HAZ metal toughness requires application of capabilities of metallurgical factor to larger extent by limitation of content of elements reducing austenite transformation temperature as well as carbide-forming elements, in particular, carbon, molybdenum, niobium etc.

1. *OTT-23.040,-KTN-314–09*: Line pipes of large diameter. General specifications.
2. (2000) *Offshore standard DNV-OS-F101*. Submarine pipeline systems. Det Norske Veritas.
3. Morozov, Yu.D., Efron, L.I. (2006) Steels for pipes of main pipelines: state-of-the-art and tendencies of development. *Metallurg*, **5**, 56–58.
4. Graf, M., Niederhoff, K. (1990) Toughness behavior of the heat-affected zone (HAZ) in double submerged-arc welded large-diameter pipe. In: *Conf. on Pipeline Technology* (15–18 Oct. 1990, Oostende, Belgium).
5. Kiryan, V.I., Semyonov, S.E. (1995) Assessment of fitness for purpose of microalloy steel welded joints of main pipelines. *Avtomatich. Svarka*, **3**, 4–9.
6. Grabin, V.F., Denisenko, A.V. (1978) *Metals science of welding of low- and medium-alloy steels*. Kiev: Naukova Dumka.
7. Hrivnak, I., Matsuda, F. (1994) Metallographic examination of martensite-austenite component (MAC) of HAZ metal of high-strength low-alloy steels. *Avtomatich. Svarka*, **3**, 22–30.
8. Terada, Y., Shinokara, Y., Hara, T. et al. (2004) High-strength line-pipes with excellent HAZ toughness. *Nippon Steel Technical Report*, **90**, 89–93.
9. Grigorenko, G.M., Kvasnitsky, V.V., Grigorenko, S.G. et al. (2009) Actual problems of investigation of physical-mechanical properties of materials for welded and brazed structures. In: *Coll. of NUK*. Mykolaiv: NUK.
10. Uwer, D., Degenkolbe, I. (1977) Kennzeichnung von Schweisstemperaturzyklen hinsichtlich ihrer Auswirkung auf die mechanischen Eigenschaften von Schweissverbindungen. *Stahl und Eisen*, **24**, 1201–1208.

Received 26.06.2013